

Extension of distance measurement range in a sinusoidal wavelength-scanning interferometer using a liquid-crystal wavelength filter with double feedback control

Osami Sasaki,^{1,*} Akihiro Saito,¹ Takamasa Suzuki,¹ Mitsuo Takeda,² and Takashi Kurokawa³

¹Faculty of Engineering, Niigata University, 8050 Ikarashi 2, Niigata-shi 950-2181, Japan

²Department of Information and Communication Engineering, The University of Electro-Communications, 1-5-1 Chofugaoka, Chofu, Tokyo 182-8585, Japan

³Graduate School of Engineering, Tokyo University of Agriculture and Technology, 2-24-16, Naka-machi, Koganei, Tokyo 184-8588, Japan

*Corresponding author: osami@eng.niigata-u.ac.jp

Received 8 May 2007; accepted 15 June 2007;
posted 29 June 2007 (Doc. ID 82805); published 9 August 2007

The optical path difference (OPD) and amplitude of a sinusoidal wavelength scanning (SWS) are controlled with a double feedback control system in an interferometer, so that a ruler marking every wavelength and a ruler with scales smaller than a wavelength are generated. These two rulers enable us to measure an OPD longer than a wavelength. A liquid-crystal Fabry-Perot interferometer (LC-FPI) is adopted as a wavelength-scanning device, and double sinusoidal phase modulation is incorporated in the SWS interferometer. Because of a high resolution of the LC-FPI, the upper limit of the measurement range can be extended to 280 μm by the use of the phase lock where the amplitude of the SWS is doubled in the feedback control. The ruler marking every wavelength is generated between 80 μm and 280 μm , and distances are measured with a high accuracy of the order of a nanometer in real time. © 2007 Optical Society of America

OCIS codes: 120.3180, 120.3930, 120.5050, 120.5060, 230.3720.

1. Introduction

Single-wavelength interferometers are limited to measurements of displacement in which a change of the optical path difference (OPD) between two measuring points is smaller than a wavelength. To overcome this limitation, two-wavelength interferometers [1–3] and wavelength-scanning interferometers [4–8] have been developed. Among these interferometers, sinusoidal wavelength-scanning interferometers are the most useful and attractive because sinusoidal wavelength scanning (SWS) can be carried out easily and exactly. Moreover, SWS is unique in that it produces a time-varying interference signal that contains a phase-modulation amplitude Z_b due to the SWS besides the conventional phase α . By processing the interference signal with a computer to calculate the values of Z_b

and α , and OPD longer than a wavelength can be measured with a high accuracy of the order of a nanometer [8]. On the other hand, operation of the phase lock can be easily carried out with a feedback control system [9] for the interference signals produced by sinusoidal-phase modulation or SWS. By keeping the two values of Z_b and α at specified values with double feedback control, a ruler marking every wavelength and a ruler with scales smaller than a wavelength are generated in the SWS interferometer. These two rulers enable us to measure an OPD longer than a wavelength in real time [10].

In this paper characteristics of the SWS interferometer with double feedback control are improved. First a liquid-crystal Fabry-Perot interferometer (LC-FPI) [11] is adopted as a wavelength-scanning device that transmits a portion of the broad light spectrum of a superluminescent diode (SLD). A vibrating slit was used to transmit a portion of the spectrum of a SLD that was generated with a diffractive grating and a

lens in Ref. [10]. Since the slit was vibrated with a speaker to produce the SWS, the resolution in the SWS was about 0.03 nm. This resolution limited the upper value of the measurable OPD to about 100 μm . Since the LC-FPI provides a high resolution in the SWS, it is expected that the upper limit is extended to a few hundreds of microns in OPD. Next, when the LC-FPI is used, frequency f_b of the SWS becomes smaller. The feedback signal for the phase lock of α was generated by using a low pass filter whose cutoff frequency was $f_b/10$ in Ref. [10]. This signal generation makes the frequency bandwidth of the feedback control system very narrow in the use of the LC-FPI. A method using double sinusoidal phase modulation [12] is incorporated in which the frequency bandwidth becomes f_b . Finally the phase lock of $Z_b = 2\pi$ is introduced in addition to the phase lock of $Z_b = \pi$ that was used in Ref. [10]. The new phase lock also extends the upper limit of the measurement range. In experiments it is shown that a ruler marking every wavelength is generated between 80 μm and 280 μm in OPD by using the LC-FPI and the phase lock of $Z_b = 2\pi$.

2. Interference Signal

Figure 1 shows a schematic diagram of a SWS interferometer with double feedback control. The central wavelength of the SWS light source (SWS-LS) is sinusoidally scanned, and it is expressed by

$$\lambda(t) = \lambda_0 + b \cos(\omega_b t). \quad (1)$$

The output of the SWS-LS is divided into an object beam and a reference beam with a beam splitter (BS). The position of mirror M1 is to be measured. The reference beam is reflected by reference mirror M2, which is displaced by piezoelectric transducer PZT1 and is vibrated by piezoelectric transducer PZT2. Its vibration is a sinusoidal motion of a $\cos(\omega_c t)$. The optical path difference (OPD) between the object and reference beam is L . The interference signal detected with a photodiode (PD) is given by

$$S_D(t) = A + B \cos[Z_c \cos(\omega_c t) + Z_b \cos(\omega_b t) + \alpha], \quad (2)$$

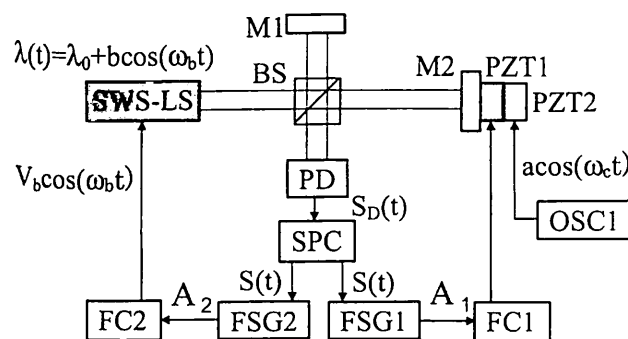


Fig. 1. Schematic diagram of sinusoidal wavelength-scanning interferometer with double feedback control for real-time distance measurement.

where A and B are constants, and

$$Z_c = 4\pi a / \lambda_0, \quad (3)$$

$$Z_b = (2\pi b / \lambda_0^2) L, \quad (4)$$

$$\alpha = -(2\pi / \lambda_0) L. \quad (5)$$

Since scanning amplitude b is very small compared to central wavelength λ_0 , $\lambda(t)$ is approximated as λ_0 in Eq. (3), and an approximation of $1/\lambda(t) = (1/\lambda_0) - [b \cos(\omega_b t) / \lambda_0^2]$ is used to derive Eqs. (4) and (5). Putting $\phi(t) = Z_b \cos \omega_b t + \alpha$, Eq. (2) is expressed as

$$S_D(t) = A + B \cos \phi(t) [J_0(Z_c) - 2J_2(Z_c) \cos 2\omega_c t + \dots] - B \sin \phi(t) [2J_1(Z_c) \cos \omega_c t + 2J_3(Z_c) \cos 3\omega_c t + \dots], \quad (6)$$

where J_n is the n th-order Bessel function.

$S_D(t)$ is multiplied by $\cos(\omega_c t)$, and we use a low pass filter in signal processing circuits SPC to extract frequency components around ω_c in the condition of $\omega_b < \omega_c$ from signal $S_D(t)$. We obtain the following interference signal to be used for double feedback control:

$$S(t) = C \sin[Z_b \cos(\omega_b t) + \alpha], \quad (7)$$

where $C = -2BJ_1(Z_c)$. The amplitude a of the vibration in Eq. (3) is adjusted so that $J_1(Z_c)$ has a maximum value.

3. Measurement Principle

First, it is explained how to measure a fractional value of OPD L with a feedback control. Sampling $S(t)$ at $\cos \omega_b t = 0$ with sample holders in feedback signal generator FSG1 produces a feedback signal

$$A_1 = C \sin \alpha, \quad (8)$$

whose frequency bandwidth is allowed to be $\omega_b/2\pi$. Feedback controller FC1 produces voltage V_α applied to the PZT1. The feedback system controls the position of reference mirror M_R or the OPD so that the feedback signal A_1 becomes zero. A change in the OPD caused by this feedback control is illustrated in Fig. 2. First the OPD is L and the position of signal A_1 is at point Q . The position of signal A_1 is moved to a stable point P by the feedback control. Phase α becomes $2m\pi$, where m is an integer. The OPD at the stable point of the feedback control is given by

$$L_z = L - L_\alpha = m\lambda_0. \quad (9)$$

L_α is a fractional value of OPD L to be measured. The range of L_α is approximately between $-\lambda_0/2$ and $\lambda_0/2$. When a change ΔV_α is detected in V_α after an OPD L is given, $L_\alpha = \beta \Delta V_\alpha$ is obtained. Constant β means a change in OPD L for a change of 1 voltage in V_α . The

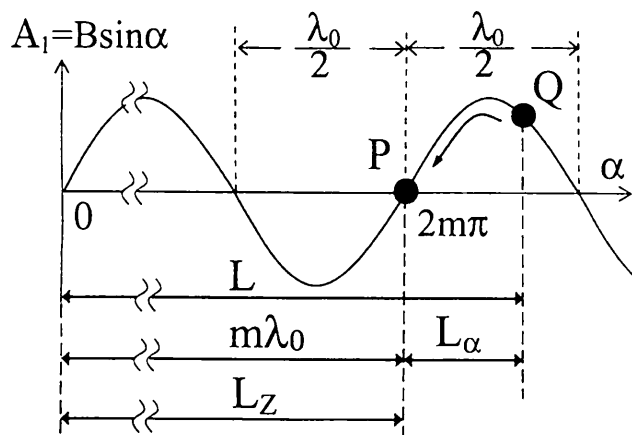


Fig. 2. Change in the OPD by feedback control, which keeps phase α at $2m\pi$.

measurement accuracy of L_a is of the order of nanometers.

Next, it is explained how to measure an integer multiple of the wavelength in the OPD L . Since the phase α is kept at $2m\pi$ by feedback control, the interference signal is

$$S(t) = C \sin[Z_b \cos(\omega_b t)], \quad (10)$$

where

$$Z_b = (2\pi b / \lambda_0^2) L_z. \quad (11)$$

Signal $S(t)$ is sampled with sample holders when $\cos \omega_b t = 1$ and $\cos \omega_b t = -1$ so that signals $S_1 = B \sin Z_b$ and $S_{-1} = -B \sin Z_b$ are obtained. From these signals a feedback signal

$$A_2 = S_{-1} - S_1 = -2B \sin Z_b \quad (12)$$

is generated in feedback signal generator FSG2. Feedback controller FC2 produces amplitude V_b of the signal applied to a wavelength-tunable filter contained in the SWS-LS. The feedback system controls the amplitude V_b or the amplitude b of the wavelength scanning so that the signal A_2 becomes zero. The feedback signal given by Eq. (12) makes modulation amplitude Z_b equal to $p\pi$, where p is equal to 1 or 3 as shown in Fig. 3(a). When the value of Z_b is less than 2π , the phase lock of $Z_b = \pi$ is produced. When the sign of the feedback signal A_2 given by Eq. (12) is inverted, the phase lock of $Z_b = p\pi$ is produced, where p is equal to 2 or 4 as shown in Fig. 3(b).

When $Z_b = p\pi$ is satisfied by the phase lock, Eqs. (9) and (11) lead to

$$b = p\lambda_0^2 / 2L_z = p\lambda_0 / 2m. \quad (13)$$

The values of b are discrete, corresponding to the values of m . Since amplitude b is proportional to amplitude V_b with a form of $b = D_1 V_b + D_0$, the values of V_b are also discrete. These discrete values of the

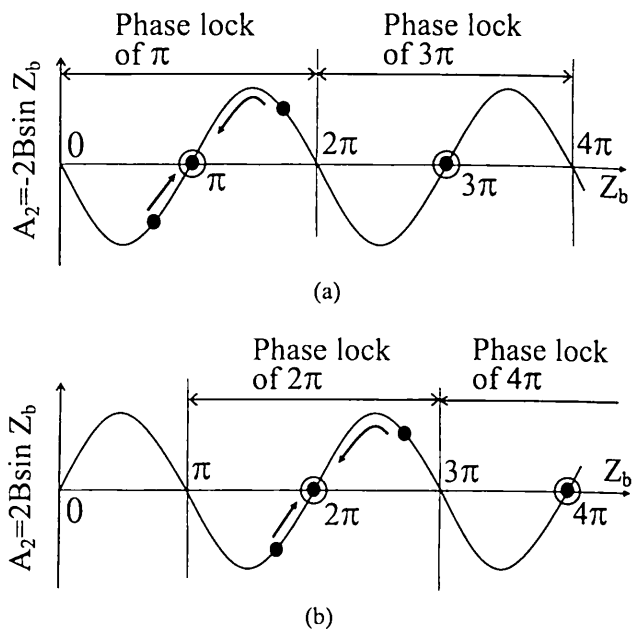


Fig. 3. Regions of Z_b where the phase lock of $Z_b = p\pi$ occurs when the feedback signal is (a) $A_2 = -2B \sin Z_b$ and (b) $A_2 = 2B \sin Z_b$.

amplitude V_b at which Z_b is equal to $p\pi$ are referred to as stable points of V_b . Since the stable points of V_b correspond to the values of m , the stable points are regarded as a ruler marking every wavelength. On the other hand, the voltage V_a is regarded as a ruler with scales smaller than a wavelength. The calibration of the ruler produced by the stable points of V_b can be made automatically by double feedback control by changing the OPD at intervals of approximately a wavelength.

When the relation of $b = D_1 V_b + D_0$ is known beforehand, the value of b is obtained from the value of V_b detected at the stable point, and a measured value of L_z is calculated by the relation of $L_z = p\lambda_0^2 / 2b$. Since L_z is given by Eq. (9), the following value is calculated by using the measured value of L_z :

$$m_c = L_z / \lambda_0. \quad (14)$$

Integer m can be decided by rounding off the value of m_c to an integer if a measurement error of L_z is smaller than $\lambda_0 / 2$. Therefore, the OPD is obtained as follows:

$$L = m\lambda_0 + L_a. \quad (15)$$

4. Extension of Measurement Range

When a stable point of V_b at L_z moves to the adjacent stable point of $V_b + \Delta V_b$ due to increasing the OPD by about a wavelength, the following change Δb in the wavelength-scanning amplitude b occurs:

$$\Delta b = -(p\lambda_0^3 / 2L_z^2). \quad (16)$$

The measurement range of the OPD is estimated theoretically from Eqs. (13) and (16) as follows: The

lower and upper limits of the measurable OPD depend on a maximum value and the resolution of the wavelength-scanning amplitude, respectively. Thus characteristics of the wavelength-tunable filter used in the SWS-LS are very important for determination of the measurement range.

In a case of $p = 1$, $L_z = 100 \mu\text{m}$, and $\lambda_0 = 840 \text{ nm}$, Eqs. (13) and (16) lead to $b = 3.5 \text{ nm}$ and $\Delta b = 0.03 \text{ nm}$. The change ΔV_b in a stable point of V_b corresponding to the change $\Delta b = 0.03 \text{ nm}$ is roughly equal to $V_b \times 10^{-3}$ in the relation of $b = D_1 V_b + D_0$. Fluctuation of the value of V_b in experiments must be so small that the value of V_b does not drift to the value of $V_b + \Delta V_b$. It is desirable that a value of ΔV_b or Δb is increased to clearly distinguish between the two different values of the adjacent stable points. To meet this requirement, the phase lock of $Z_b = p\pi$ ($p = 2, 3, \dots$) is adopted instead of the phase lock of $Z_b = \pi$. When the value of Δb is enlarged p times by adopting the phase lock of $Z_b = p\pi$, an upper limit of the measurable OPD can be increased by $p^{1/2}$.

5. Experimental Setup

The SWS interferometer shown in Fig. 1 has been constructed. The schematic illustration of the SWS-LS is shown in Fig. 4. A SLD was used as a broadband light source whose central wavelength λ_0 and spectral bandwidth were 844.26 nm and 20 nm, respectively. The output from the SLD was collimated with lens L1, and the diameter of the collimated beam was about 3 mm. A liquid-crystal Fabry–Perot interferometer (LC-FPI) was used as a wavelength-tunable filter. The LC-FPI transmits a very narrow spectrum whose bandwidth is 1.4 nm and whose central wavelength is tuned by a voltage applied to the LC-FPI. The tuned wavelength is varied from 820 nm to 860 nm for static tuning. The LC-FPI was placed in a focal plane of lens 2 whose focal length was 50 mm. A voltage of $V_b \cos(\omega_b t)$ was applied to the LC-FPI to produce a sinusoidal wavelength scanning of $\lambda(t) = \lambda_0 + b \cos(\omega_b t)$. The frequency of $\omega_b/2\pi$ was 120 Hz. The light transmitted by the LC-FPI was collimated with lens L3 and was split by a polarizer beam splitter (PBS) into two light beams. One of them was wavelength scanned and was used as the output of the SWS-LS for the interferometer.

Sinusoidal vibration frequency $\omega_c/2\pi$ of the reference mirror M2 was $64 \times (\omega_b/2\pi) = 7.68 \text{ kHz}$. The vibration amplitude was adjusted so that $J_1(Z_c)$ became a maximum value. Change L_a in the OPD pro-

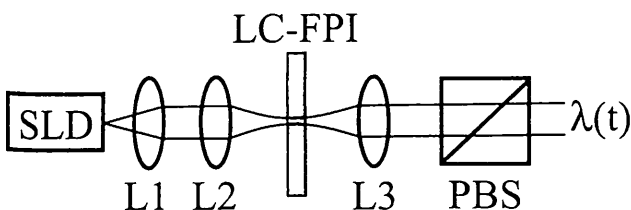


Fig. 4. Schematic illustration of the sinusoidal wavelength-scanning light source (SWS-LS) using a liquid-crystal Fabry–Perot interferometer (LC-FPI).

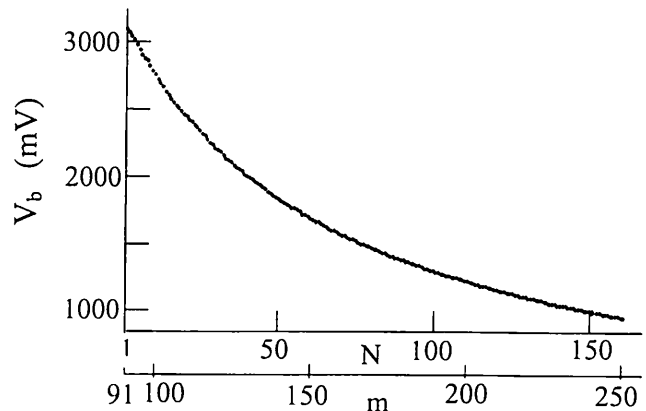


Fig. 5. Stable points of V_b obtained at the phase lock of $Z_b = \pi$. N is the number of the stable points. The stable point is assigned to the number m in which $L_z = m\lambda_0$.

vided by the displacement of the reference mirror was expressed by $L_a = \beta \Delta V_a$, where $\beta = 83.37 \text{ nm/V}$. Mirror M1 fixed on a stage was used as an object.

6. Experimental Results

When changes in OPD L were made at intervals of one wavelength by utilizing the feedback control of OPD at a fixed value of V_b , values of Z_b were calculated from the interference signal given by Eq. (2) with a computer by the method of double sinusoidal phase modulating interferometry described in Ref. [12]. Three values of b at $V_b = 1.0 \text{ V}$, 1.5 V , and 2.0 V were obtained from the values of Z_b calculated for the changes in L , and finally the relation of b [nm] = $1.47 V_b$ [V] + 0.31 was obtained.

Displacements were given to the object with a micrometer to change the OPD. By increasing the OPD at intervals of about one wavelength, a stable point of V_b could be moved to the next point automatically. 160 stable points of V_b were obtained at the phase lock of $Z_b = \pi$ as shown in Fig. 5, whose horizontal axis is the number N of the stable point. These values of V_b at the stable points were converted into values of b with the relation between b and V_b to obtain measured values of $L_z = \lambda_0^2/2b$. Values of m_c were calculated from the measured values of L_z with Eq. (14). Since the absolute value of the difference between the value of m_c and an integer of its round

Table 1. Measured Values at the Phase Lock of $Z_b = \pi$

V_b [mV]	b [nm]	L_z [μm]	m_c	m
2217	3.57	99.842	118.3	118
2198	3.54	100.630	119.2	119
2179	3.51	101.430	120.1	120
1412	2.39	149.367	176.9	177
1400	2.37	150.480	178.3	178
1391	2.36	151.326	179.3	179
980	1.751	203.551	241.1	241
976	1.745	204.237	241.9	242
972	1.739	204.928	242.7	243

Table 2. Measured Values at the Phase Lock of $Z_b = 2\pi$

V_b [mV]	b [nm]	L_Z [μm]	m_c	m
2175	3.51	203.200	240.7	241
2165	3.49	204.055	241.7	242
2154	3.48	205.005	242.8	243
1523	2.55	279.610	331.2	331
1518	2.54	280.419	332.2	332
1513	2.53	281.232	333.1	333

number was less than 0.5 in the region of $N = 20$ – 140 , values of integer m and the relation of $m = N + 90$ could be determined as shown in Fig. 5. Table 1 shows the values of b , L_Z , m_c , and m for some stable points in the different regions around $L_Z = 100 \mu\text{m}$, $150 \mu\text{m}$, and $200 \mu\text{m}$. Since the magnitude of the fluctuations in values of the stable points with time was close to the value of Δb around $L_Z + 200 \mu\text{m}$, about $200 \mu\text{m}$ was the upper limit of the measurable OPD at the phase lock of $Z_b = \pi$. It is estimated that the resolution of the wavelength scanning is higher than the value of Δb given by Eq. (16) at $L_Z = 204 \mu\text{m}$, that is, 0.007 nm .

The sign of the feedback signal A_2 was inverted at the stable point of $V_b = 980 \text{ mV}$ shown in Table 1 for the phase lock of $Z_b = 2\pi$ to start. The values of the stable points around $L_Z = 200 \mu\text{m}$ at the phase lock of $Z_b = \pi$ shown in Table 1 were changed to the values shown at Table 2. The same values of m were obtained, although the values of L_Z or m_c changed a little. The results made it clear that using the phase lock of $Z_b = 2\pi$ enlarges the values of ΔV_b about two times. Stable points for up to $L_Z = 280 \mu\text{m}$ could be obtained as shown at Table 2.

Finally, displacement D of mirror $M1$ was measured that was given with the micrometer. Values of V_b and ΔV_a are detected as shown at Table 3, where the phase lock of $Z_b = \pi$ was switched to the phase lock of $Z_b = 2\pi$ at $2D = 100 \mu\text{m}$. The value of m was decided by the relation between the stable points of V_b and the values of m . The value of L_a was calculated with $L_a = 83.37\Delta V_a$. ΔL was the difference between the two values of OPD measured successively. There were differences between $2D$ and ΔL because the displacement given by the micrometer was not so accu-

Table 3. Results of Distance Measurement

$2D$	V_b [mV]	m	ΔV_a [V]	L_a [μm]	L [μm]	ΔL
0	2302	114	3.9	0.325	95.564	
50	1437	174	-4.3	-0.358	146.533	49.969
100	1021	233	0.4	0.033	196.733	50.200
100	2251	233	0.4	0.033	196.733	
150	1748	293	3.4	0.283	247.635	50.902
180	1550	326	4.9	0.409	275.619	27.984

rate. Since the measurement error in ΔV_a was estimated to be less than 0.05 V , the measurement error in L_a was less than 4 nm .

7. Conclusion

The liquid-crystal Fabry–Perot interferometer (LC-FPI) was adopted as a wavelength-scanning device in the SWS interferometer with double feedback control. By incorporating double sinusoidal phase modulation, a better interference signal was obtained from which the feedback signal with frequency bandwidth equal to the frequency of the SWS could be generated. Because of the high resolution of the LC-FPI, the upper limit of the measurement range was obtained at $200 \mu\text{m}$ at the phase lock of $Z_b = \pi$. Moreover, the phase lock of $Z_b = 2\pi$ was used instead of $Z_b = \pi$ in the region longer than $200 \mu\text{m}$, so that the upper limit of the measurement range became $280 \mu\text{m}$. The measurement range was from $80 \mu\text{m}$ to $290 \mu\text{m}$ with the measurement error less than 4 nm .

References

1. P. de Groot and S. Kishner, "Synthetic wavelength stabilization for two-color laser-diode interferometry," *Appl. Opt.* **30**, 4026–4033 (1991).
2. R. Onodera and Y. Ishii, "Two-wavelength laser-diode interferometer with fractional fringe techniques," *Appl. Opt.* **34**, 4740–4746 (1995).
3. T. Suzuki, K. Kobayashi, and O. Sasaki, "Real-time displacement measurement with a two-wavelength sinusoidal phase-modulating laser diode," *Appl. Opt.* **39**, 2646–2652 (2000).
4. S. Kuwamura and I. Yamaguchi, "Wavelength scanning profilometry for real-time surface shape measurement," *Appl. Opt.* **36**, 4473–4482 (1997).
5. F. Lexer, C. K. Hitzenberger, A. F. Fercher, and M. Kulhavy, "Wavelength-tuning interferometry of intraocular distances," *Appl. Opt.* **36**, 6548–6553 (1997).
6. T. Li, R. G. May, A. Wang, and R. O. Claus, "Optical scanning extrinsic Fabry–Perot interferometer for absolute microdisplacement measurement," *Appl. Opt.* **36**, 8859–8861 (1997).
7. X. Dai and K. Seta, "High-accuracy absolute distance measurement by means of wavelength scanning heterodyne interferometry," *Meas. Sci. Technol.* **9**, 1013–1035 (1998).
8. O. Sasaki, N. Murata, and T. Suzuki, "Sinusoidal wavelength-scanning interferometer with a superluminescent diode for step-profile measurement," *Appl. Opt.* **39**, 4589–4592 (2000).
9. T. Suzuki, O. Sasaki, and T. Maruyama, "Phase-locked laser diode interferometry for surface profile measurement," *Appl. Opt.* **28**, 4407–4410 (1989).
10. O. Sasaki, K. Akiyama, and T. Suzuki, "Sinusoidal-wavelength-scanning interferometer with double feedback control for real-time distance measurement," *Appl. Opt.* **41**, 3906–3910 (2002).
11. M. Kinoshita, M. Takeda, H. Yago, Y. Watanabe, and T. Kurokawa, "Optical frequency-domain microprofilometry with a frequency-tunable liquid-crystal Fabry–Perot etalon device," *Appl. Opt.* **38**, 7063–7068 (1999).
12. O. Sasaki, T. Yoshida, and T. Suzuki, "Double sinusoidal phase-modulating laser diode interferometer for distance measurement," *Appl. Opt.* **30**, 3617–3621 (1991).